

ORIGINAL RESEARCH PAPER

## Photocatalytic degradation study of Methyl Orange and Congo red using Mg-Co ferrite powder

S. D. Jadhav\*, R. S. Patil

Department of Chemistry, Yashwantrao Chavan College of Science, Karad Shivaji University, Kolhapur, (MH) India.

Received: 2022-03-05

Accepted: 2022-04-25

Published: 2022-05-01

### ABSTRACT

The photocatalytic degradation of methyl orange and Congo red dye was performed under the illumination of visible light (Philips 250Watt) as a source of photons. The complete distraction of the aromatic ring was ascertained by UV spectroscopic analysis. A decrease in dye concentration and an increase in the concentration of CO<sub>2</sub> indicate dye mineralization. The behavior of this reaction was pseudo-first-order and the maximum photodecolorization efficiency was ~85.16% for Methyl orange and ~ 95.40 for Congo red in 120-150 min. at 30°C.

**Keywords:** Ferrite, Co-precipitation, X-ray Diffraction, Scanning electron microscopy, Transmission electron microscopy (TEM), Photodegradation of dye.

### How to cite this article

Jadhav S. D., Patil R. S. Photocatalytic degradation study of Methyl Orange and Congo red using Mg-Co ferrite powder. *J. Water Environ. Nanotechnol.*, 2022; 7(2): 170-179.  
DOI: 10.22090/jwent.2022.02.005

### INTRODUCTION

Water contamination is mainly caused due to toxic effluents drained by several chemicals, in agricultural and textile industries. It has been reported that about 25% of dyestuffs are discharged directly into the environment by the textile factory. Generally, wastewater generated by the textile industry contains a considerable amount of non-fixed dyes, especially azo dyes, and a huge amount of inorganic salts. Also contains several non-biodegradable substrates that could be harmful to the environment. Their toxicity, stability to natural decomposition, and persistence in the environment have been the cause of much concern to society and regulation authorities all around the world [1-4]. Environmental problems associated with toxic organic pollutants in water and air are the current issue to be solved for the development of a healthy environment.

Photocatalytic oxidation is one of the emerging

technologies for the decomposition of organic dyes such as Reactive black 5, Acid orange, Aniline yellow, Orange B, Methyl yellow, Methyl red, Methylene blue, Congo red & Methyl orange, etc. Azo dyes represent about one-half of the dyes used in the textile industry. Among azo dyes, Methyl Orange (MO) is highly water-soluble, even at very low concentrations, which hinders the penetration of light and therefore causes adverse effects on photosynthesis. Congo Red (CR) was the first synthetic dye that could dye cotton directly [5]. It is contained in wastewater effluents from the textile, printing and dyeing, paper, rubber, and plastics industries. CR is used in medicine as a biological stain and as an indicator since it turns from red-brown in a basic medium to blue in an acidic one. These are the different ways organic pollutants (dyes) continuously get added to water sources. The incomplete decomposition of organic pollutants may lead to the formation of more toxic byproducts than the parent pollutants. Therefore, to overcome such a problem, looking for a metal

\* Corresponding Author Email: [sdjchemsuk@gmail.com](mailto:sdjchemsuk@gmail.com)

oxide photocatalyst with a strong photodegradation capacity is inevitable.

For instance, Jang et al. [6] and Jung et al. [7] respectively demonstrated that  $ZnFe_2O_4$  and  $CaFe_2O_4$  systems are useful for solar photocatalytic degradation of pollutants. Similarly, in the case of homo [8] or hetero [9] composite ferrite systems,  $CaFe_2O_4:MgFe_2O_4$  and  $ZnFe_2O_4:SrTiO_3$  are efficient and useful for photocatalytic water splitting. It has been reported that Ching Cheng *et al* [10] investigated the effects of cation distribution in  $CdFe_2O_4$ , M. Yokoyama *et al* [11] studied the magnetic properties of cadmium ferrite prepared by coprecipitation, Ashok Gadkaria *et al* [12] reported on structural and magnetic properties of  $CdFe_2O_4$  ferrites, Silva *et al.* [13] reported the magnetic resonance investigation of cadmium ferrite. Cai et al. developed  $ZnFe_2O_4$  via a reduction-oxidation method which showed the degradation of Orange II dye [14], Sharma et al.  $MFe_2O_4$  (M=Co, Ni, Cu, Zn) prepared by the sol-gel method used for Methyl blue dye degradation [15], Dhiman et al. reported  $NiFe_2O_4$  visible light assisted photocatalytic degradation of Safranin - O dye and remazol brilliant yellow at pH 2.5 [16]. S. D. Jadhav et al. used  $ZnFe_2O_4$  for the degradation of Methyl orange dye [17]. Hankare et al. studied  $CoFe_2O_4$  prepared by sol-gel method for methylene blue degradation [18]. The ferrites offer an advantage of displaying the desirable optical absorption for the low-energy photons ( $h\nu \sim 2eV$ ), and of exhibiting the well-suited electronic structure desirable for photocatalytic applications [19]. This contrasts with the very popular anatase  $TiO_2$  reference material, whose band gap of 3.2 eV allows only the absorption of UV light, corresponding to wavelengths lower than 388 nm [20].

On the other hand, photocatalysts are non-magnetic such as semiconductors ( $TiO_2$ , ZnO, and ZnS), and their separation and recovery after the treatment are difficult [21]. Consequently, the problem of insufficient recovery not only leads to the loss of photocatalysts but also the residual photocatalyst causes additional environmental problems. Therefore, the effective and complete decolorization of organic pollutants containing wastewater is an important and challenging task. To make full use of solar energy, many attempts have been made to prepare the narrow band gap ferrite semiconducting material that utilizes the much larger visible region. Some of the recent reports could be important indicators with respect to the

potential of visible light photocatalytic application of the spinel ferrites. Spinel ferrites which are mixed oxides of iron and a single or numerous metals are one such example of visible-light absorbing inorganic semiconductors studied for their photocatalytic activity due to their attractive photochemical properties such as narrow optical band gap ( $\sim 2.0eV$ ), good photochemical stability [22] and the recovery of photocatalysts and their relative stability in acidic and basic conditions [23]. They not only have strong photodegradation capacities but also improve the degradation rate of pollutants and ease the reaction mixture form after being used; Consequently, making them very useful for the complete removal of organic pollutants [24-26].

To the best of our knowledge, as per the literature, few reports have been cited in the literature on the photocatalytic properties of divalent metal ion-doped cobalt ferrite nanoparticles under solar light irradiation. Accordingly, in this paper, we reported photocatalytic degradation of azo dye using magnesium doped cobalt ferrite nanoparticles.

## EXPERIMENTAL

### Materials

Methyl orange and Congo red dye were supplied by Sigma Aldrich which is a Physico-chemical characteristic that is illustrated in **Fig. 1 and Table 1**.

### Method

The Mg-Co ferrite has been synthesized by using a controlled co-precipitation technique [27]. The setup for the decolorization of organic dyes and the basics of photoreaction is shown in **Fig. 3**. The series of the photoreaction experiments were conducted by mixing 100 mL of an aqueous solution of Methyl orange and Congo red with a suitable amount of  $Mg_{0.5}Co_{0.5}Fe_2O_4$  nanopowder as suspension solution. The equilibrium time for this reaction was closely performed at 30 min as the adsorption process. Visible light bulbs containing tungsten filament (Philips 250 W) were applied as a source of photons; it was connected at the top of the reactor chamber [28]. Light intensity value equal to  $1.48 \times 10^{-7}$  Ens.  $s^{-1}$ , which is calculated by a chemical actinometrical solution [29]. At regular intervals, a certain amount of samples were collected and double separated by centrifuge to remove all photocatalyst from dye solutions. The filtered dye solutions were analyzed to determine

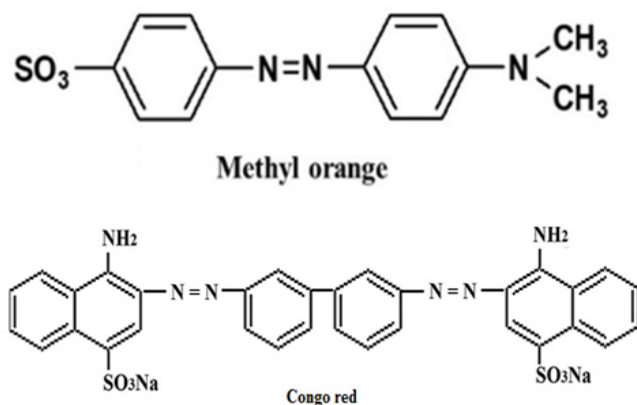


Fig. 1. The structural formula of Methyl orange and Congo red dye.

Table 1. Physico-chemical characteristics of the Methyl orange and Congo red dye.

Parameters	Methyl orange	Congo red
Synonym	547-58-0 Orange III	Direct red 28.
Molecular Weight	327.33g/mol	696.665g/mol
Molecular formula	C <sub>14</sub> H <sub>14</sub> N <sub>3</sub> O <sub>3</sub> SNa	C <sub>32</sub> H <sub>22</sub> N <sub>6</sub> Na <sub>2</sub> O <sub>6</sub> S <sub>2</sub>
Type	Acid dye	Acid-Basic Indicator
λ <sub>max</sub>	460-470 nm	497-498 nm
Solubility in water	Soluble	Soluble

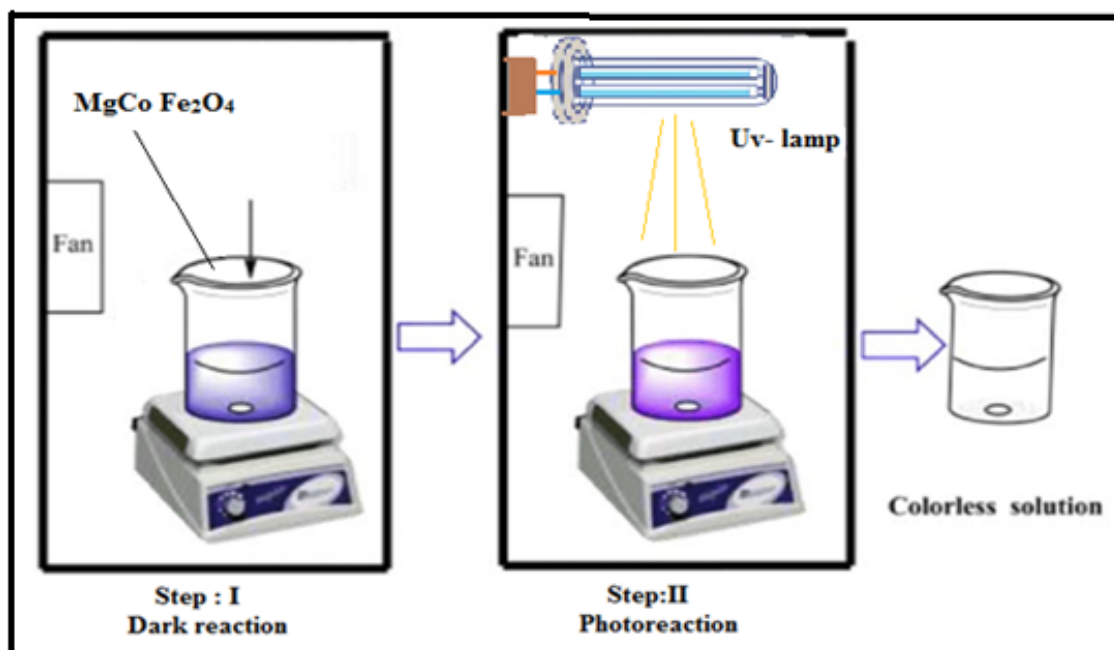


Fig. 2. Setup for reaction in dark and reaction in light.

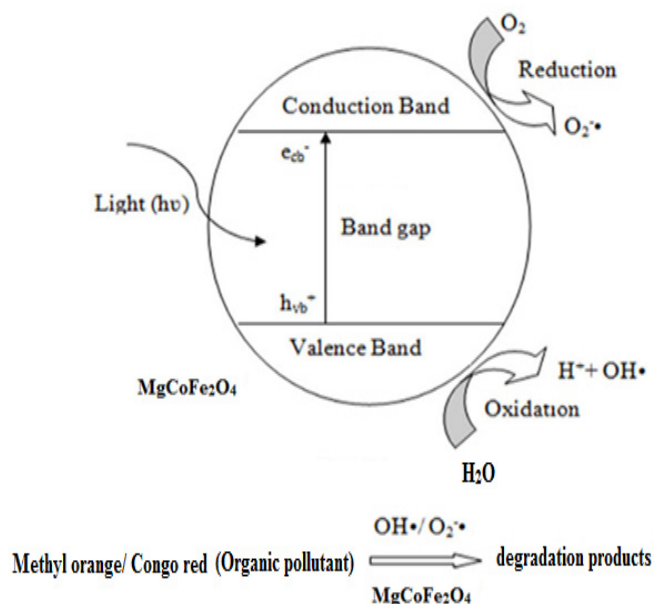


Fig. 3. Setup for decolorization of organic dyes and basics of photoreaction

the residue concentration of dye by recording the absorbance at 464 nm and 500nm using a UV visible spectrophotometer.

By being dependent on the Langmuir-Henselwood mechanism, the rate constant was determined [30], and the photodecolorization efficiency (PDE %) was calculated by the following equation [31].

$$\ln(C_0/C_t) = K_{app} \cdot x \cdot t \quad (1)$$

$$PDE\% = \frac{C_0 - C_t}{C_0} \times 100 \quad (2)$$

Here: C<sub>0</sub> is an initial concentration of methyl Orange and Congo red dyes at no irradiation time (min). C<sub>t</sub> is a concentration of the same dye at t time of irradiation (min).

## RESULTS AND DISCUSSION

### Characterization

The X-ray diffraction patterns of the system Mg<sub>1-x</sub>Co<sub>x</sub>Fe<sub>2</sub>O<sub>4</sub> (x = 0.0 to 1.0) sintered at 600°C as shown in Fig. 4. All the indexed diffraction peaks correspond to the (111), (220), (311), (400), (422), and (511) planes of polycrystalline spinel ferrite [32]. The X-ray lines were found to be sharp which makes detection of the phases easy. All spinel composition indicates the (311) peak is the more intense one. The crystallite size and porosity of the resulting ferrite powder were 38 and 10.52nm,

respectively. The d<sub>hkl</sub> and 2θ values were compared with the values reported in the literature (cubic, MgFe<sub>2</sub>O<sub>4</sub>, JCPDS file No. 73-1720) and (cubic, CoFe<sub>2</sub>O<sub>4</sub>, JCPDS file No. 22-1086).

The SEM micrograph shows the formation of polycrystalline grains. From this image, it could be seen that most of the grains have a size of about 5 microns Fig. 5 (a). Transmission electron micrographs of the Mg<sub>0.5</sub>Co<sub>0.5</sub>Fe<sub>2</sub>O<sub>4</sub> system are depicted in Fig. 5(b & c). The corresponding selected area electron diffractograms (SAEDs) are given as an inset. It is evident from this micrograph that the synthesized powder particles were ~200 nm in size. The superimposition of the bright spot with the Debye ring pattern indicates the polycrystalline nature of the sample.

### Effect of irradiation time on photodegradation of Methyl orange and Congo red dyes.

To test the photocatalytic (PC) properties of Mg<sub>0.5</sub>Co<sub>0.5</sub>Fe<sub>2</sub>O<sub>4</sub>, the degradation kinetics of a pollutant model, methyl orange (MO), and Congo red (CR) were followed in water, under visible light (250W) illumination. The intensity of the characteristic absorption bands of MO & CR centered at about 460-470 nm and 498- 502nm respectively [33], was measured every 30 min. The degradation of MO solution was selected as a reference and the characteristic absorption of MO solution at about 464 nm was selected for

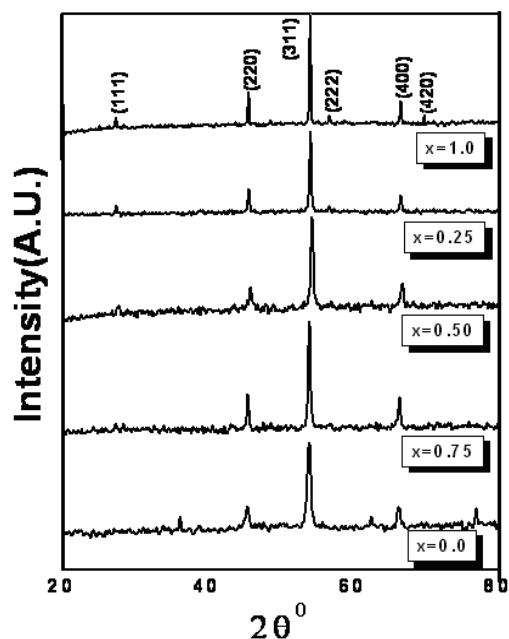


Fig. 4. XRD Patterns for the  $Mg_{1-x}Co_xFe_2O_4$  system sintered at  $600^\circ C$  ( $0 \leq x \leq 1$ ).

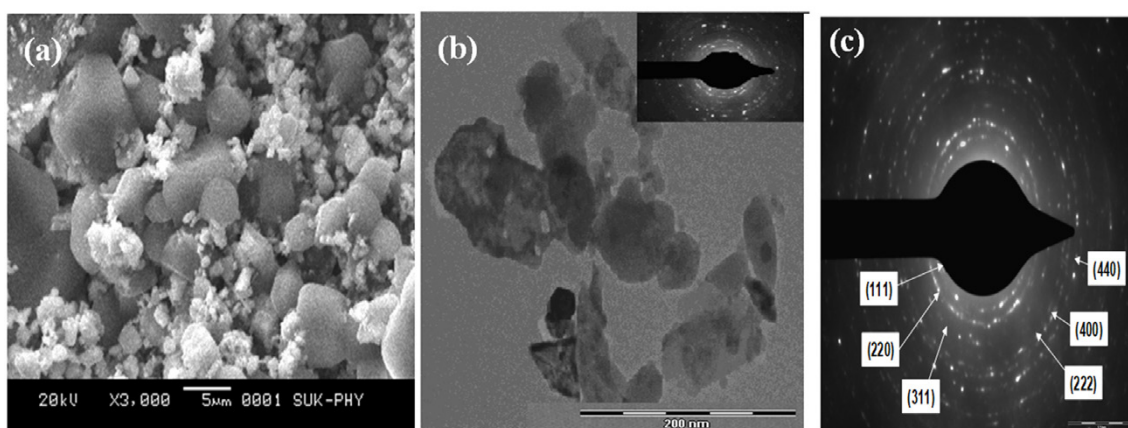


Fig.5. (a) Scanning electron micrograph (b) Transmission electron micrograph (c) SAED pattern for  $Mg_{0.5}Co_{0.5}Fe_2O_4$  sintered at  $600^\circ C$ .

monitoring the adsorption and photocatalytic degradation process. A significant decrease in transmittance at about 460 nm could be assigned to the absorption of light caused by the excitation of electrons from the valence band to the conduction band of MO solution **Fig. 6**. For CR there was complete absorption of light by CR solution, the absorption peak at 500 nm disappears and no peak shift can be detected after the degradation treatment **Fig. 7**. The further comparison reveals ~80% and ~90% degradation of methyl orange and Congo red within 120-150 min of irradiation, respectively. The increase of the pH value after

visible light irradiation is due to the reduction of surface acidic groups in the ferrite powders, which were introduced during the preparation [34].

#### *Concentration effect of dye solution on the photo decolorization rate of methyl orange and Congo red dyes.*

The effect of initial dye concentration was studied by fixing the amount of photocatalyst and other parameters only by varying the amount of dye concentration to check the photodegradation activity. Dye concentration ranges from 10 to 50 ppm. After the reaction study, the results concluded

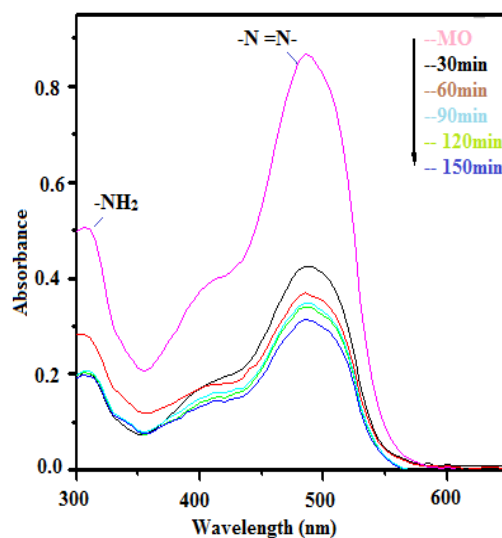


Fig. 6. Effect of irradiation time on Methyl Orange dye

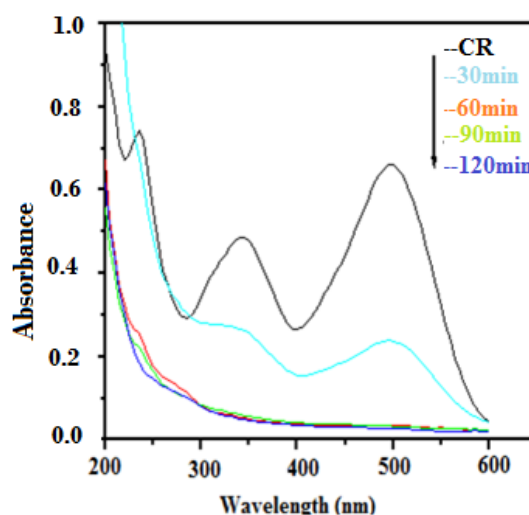


Fig. 7. Effect of irradiation time on Congo red dye

that increasing the dye concentration, in turn, decreases the photocatalyst performance as shown in Fig.8. Initially, the percent degradation of MO and CR increased up to 30ppm. This is because more amount of dye molecules come in contact with the photocatalyst surface, so the degradation amount is also high. However, when the dye concentration increased above 30ppm, the percent degradation of dyes decreased. It is generally noted that the degradation rate increases with the increase of dye concentration to a certain concentration and a further increase lead to a decrease in the dye degradation rate (Sakthivel et al. 2003)[35].

Our results agree with those previously reported (Kansal et al. 2007; Li et al. 2005)[36] that with the increase in dye concentration while irradiating the MO and CR solution, the dye percent degradation was decreased.

#### *Effect of catalyst dose on the photodecolorization rate of methyl orange and Congo red dyes.*

As seen in Fig. 9 & 10 (a) & (b), the increased doses of catalyst from the range (0.5-2.5)g in an aqueous solution of methyl orange and Congo red dyes solution raised the decolonization speed. This behavior indicates finding the many active

sites of catalyst surface with increasing the dose. The transmitted light in dye solution is easily transmitted; hence, that entirely leads to the enhancement in producing hydroxyl radical. This case will accelerate the decolorization of the dye according to the first possibility of the Langmuir-Hinshelwood (L-H) kinetics model [37]. The maximum rate constant and PDE % are found at dose 2.0 g/ 100 mL of  $Mg_{0.5}Co_{0.5}Fe_2O_4$  and 85.16% at 70 min and 95.40% at 60 min.

On the other hand, after using 2.5 mg/100 mL of catalyst powder, the rate of reaction depresses, based on the raised the solution turbidity and declined the transmittance of light, which caused inhibited hydroxyl radical formation and this effect is called the screen effect. [38-40]

#### Reusability study of catalyst

The effect of catalyst used after several runs on the dye solution at conditions: dose (2.0) g/100mL, conc. = 30 ppm, initial pH of solution = 5.5 and T= 303K. The PDE% for Methyl orange is 85.16%

and the PDE% for Congo red is 95.40%. The photodegradation rate further goes on decreases after each successive run (Fig.11 &12).

#### Mechanism

The suggested mechanism for the decolorization of methyl orange and congo red dyes was depicted in **scheme 1**. To form hydroxyl radical on  $Mg_{0.5}Co_{0.5}Fe_2O_4$  nanopowder surface must focus light on the suspension solution. Based on the photodecolorization processes described in the reference, various redox processes could be conducted on the surface of a photo semiconductor under the illumination of visible light. Firstly, electron-hole pair (exciton) on the catalyst surface was generated. The electron-hole pair was separated by reacting with other species ( $H_2O$ ,  $O_2$ ) in a series of steps and subsequently, formed groups of radical intermediates like superoxide ion  $O_2^-$  hydrogen peroxide radical (hydroperoxyl radical) then leads to hydroxyl radical which has more activity than  $HO_2^-$  [41-42].

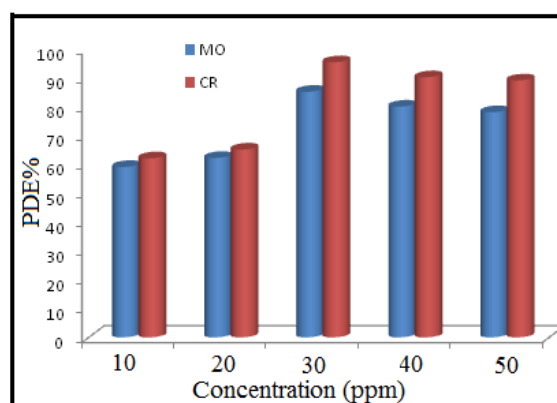


Fig. 8. Effect of concentration of dye solution on the photodecolorization rate of methyl orange and Congo red dyes.

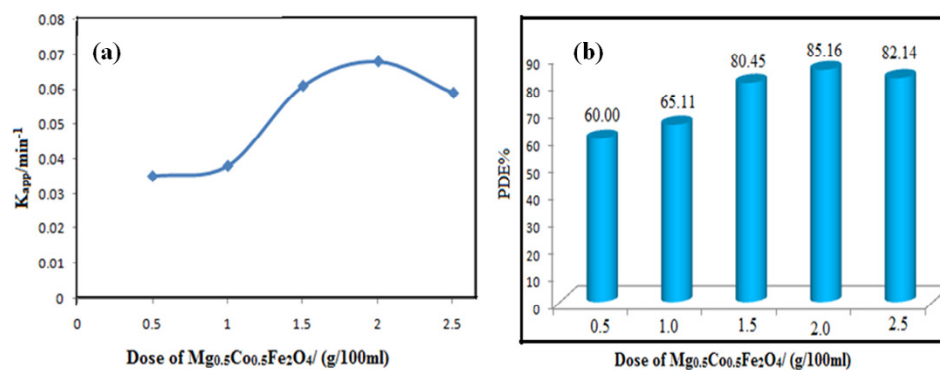


Fig. 9. Effect of catalyst dose on the (a) apparent rate constant of reaction (b) PDE %, at conditions: cat. dose = (0.5-2.5) g/100mL, methyl orange dye conc.= 30 ppm, initial pH of solution= 5.5 and T= 303K.

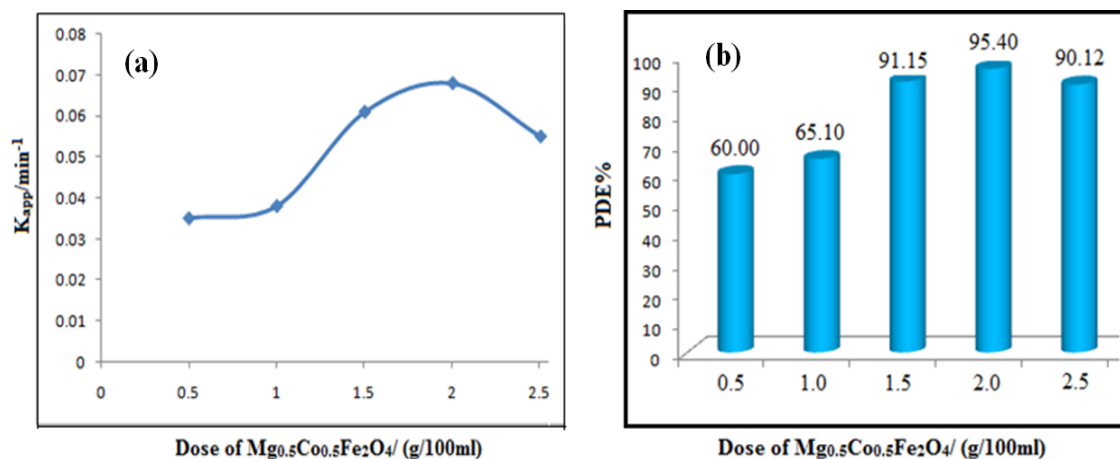


Fig.10. Effect of catalyst dose on the (a) apparent rate constant of reaction (b) PDE %, at conditions: cat. Dose = (0.5-2.5) g/100mL, Congo red dye conc.= 30 ppm, initial pH of solution= 5.5 and T= 303K

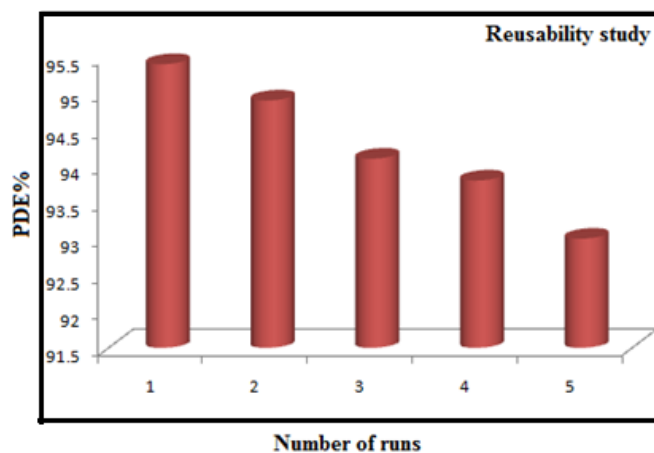


Fig.11. Reuse of catalyst at conditions: dose (2.0) g/100mL, conc.= 30 ppm, initial pH of solution= 5.5 and T= 303K for Methyl orange dye.

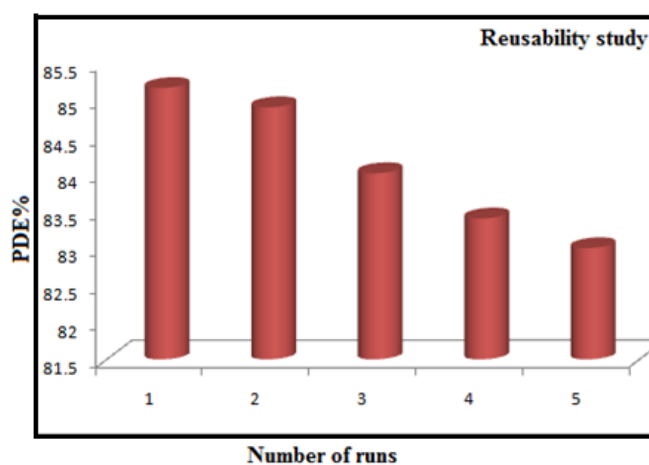
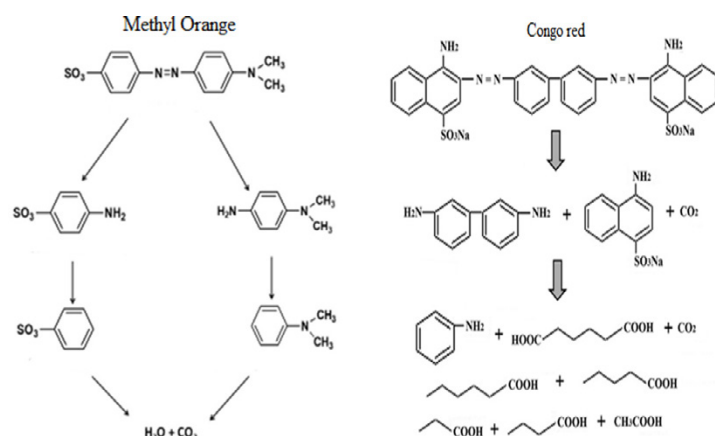


Fig.12. Reuse of catalyst at conditions: dose (2.0) g/100mL, conc. = 30 ppm, initial pH of solution= 5.5 and T= 303K for Congo red dye.



Scheme 1 Schematic diagram for accepted mechanism (methyl orange &amp; congo red dyes visible light system)

## CONCLUSION

In this study, the main conclusions were observed that the photocatalytic decolorization process of methyl orange and Congo red dyes in suspension solution of  $\text{Mg}_{0.5}\text{Co}_{0.5}\text{Fe}_2\text{O}_4$  nanopowder under a visible light system was carried out. This photoreaction is found to be endothermic and obeyed the pseudo-first-order with low activation energy. In the case of methyl orange, the rate of reaction is moderate, and the same for Congo red is fast. The PDE% for Methyl orange is 85.16% A than the PDE% of Congo red 95.40%. With further reuse of catalyst, the rate of photodegradation goes on decreases after each successive run. The suitable mechanism was suggested to obtain the depolarization and degradation of this dye with form  $\text{CO}_2$  and  $\text{H}_2\text{O}$  (mineralization process) and the final pH was maintained at 7.4.

## ACKNOWLEDGMENT

Author (SDJ) thankful to the department of chemistry, Yashwantrao Chavan College of Science, Karad.

## CONFLICT OF INTEREST

The authors declare no conflict of interest.

## REFERENCES

- [1] Shandilya, P., Sambyal, S., Sharma, R., Kumar, A., & Vo, D. V. N. (2021). Recent Advancement on Ferrite Based Heterojunction for Photocatalytic Degradation of Organic Pollutants: A Review. *Ferrite: Nanostructures with Tunable Properties and Diverse Applications*, 112, 121-161. <https://doi.org/10.21741/9781644901595-3>
- [2] Gupta, S. M., & Tripathi, M. (2011). A review of  $\text{TiO}_2$  nanoparticles. *Chinese science bulletin*, 56(16), 1639-1657. <https://doi.org/10.1007/s11434-011-4476-1>
- [3] Nguyen, L. T., Nguyen, L. T., Duong, A. T., Nguyen, B. D., Quang Hai, N., Chu, V. H., ... & Bach, L. G. (2019). Prepa-

- ration, characterization and photocatalytic activity of L-doped zinc oxide nanoparticles. *Materials*, 12(8), 1195. <https://doi.org/10.3390/ma12081195>
- [4] Gul, S., Yousuf, M. A., Anwar, A., Warsi, M. F., Agboola, P. O., Shakir, I., & Shahid, M. (2020). Al-substituted zinc spinel ferrite nanoparticles: Preparation and evaluation of structural, electrical, magnetic and photocatalytic properties. *Ceramics International*, 46(9), 14195-14205. <https://doi.org/10.1016/j.ceramint.2020.02.228>
- [5] Jadhav, S. D., & Patil, R. S. (2022). Photocatalytic degradation study of Methyl Orange and Congo red using  $\text{Mg-Co}$  ferrite powder. *Journal of Water and Environmental Nanotechnology*, 7(2), 170-179. <https://dx.doi.org/10.22090/jwent.2022.02.005>
- [6] Jang, J. S., Hong, S. J., Lee, J. S., Borse, P. H., Jung, O. S., Hong, T. E., ... & Kim, H. G. (2009). Synthesis of zinc ferrite and its photocatalytic application under visible light. *Journal of the Korean Physical Society*, 54(1), 204-208. <https://doi.org/10.3938/jkps.54.204>
- [7] Jeong, E. D., Borse, P. H., Jang, J. S., Lee, J. S., Cho, C. R., Bae, J. S., ... & Kim, H. G. (2009). Physical and optical properties of nanocrystalline calcium ferrite synthesized by the polymerized complex method. *Journal of Nanoscience and Nanotechnology*, 9(6), 3568-3573. <https://doi.org/10.1166/jnn.2009.NS31>
- [8] Kim, H. G., Borse, P. H., Jang, J. S., Jeong, E. D., Jung, O. S., Suh, Y. J., & Lee, J. S. (2009). Fabrication of  $\text{CaFe}_2\text{O}_4/\text{MgFe}_2\text{O}_4$  bulk heterojunction for enhanced visible light photocatalysis. *Chemical Communications*, (39), 5889-5891. <https://doi.org/10.1039/b911805e>
- [9] Boumaza, S., Boudjemaa, A., Bouguelia, A., Bouarab, R., & Trari, M. (2010). Visible light induced hydrogen evolution on new hetero-system  $\text{ZnFe}_2\text{O}_4/\text{SrTiO}_3$ . *Applied Energy*, 87(7), 2230-2236. <https://doi.org/10.1016/j.apenergy.2009.12.016>
- [10] Cheng, C., & Liu, C. S. (2009). Effects of cation distribution in  $\text{ZnFe}_2\text{O}_4$  and  $\text{CdFe}_2\text{O}_4$ : ab initio studies. In *Journal of Physics: Conference Series* (Vol. 145, No. 1, p. 012028). IOP Publishing. <https://doi.org/10.1088/1742-6596/145/1/012028>
- [11] Yokoyama, M., Sato, T., Ohta, E., & Sato, T. (1996). Magnetization of cadmium ferrite prepared by coprecipitation. *Journal of applied physics*, 80(2), 1015-1019. <https://doi.org/10.1063/1.362834>
- [12] Gadkari, A., Shinde, T., & Vasambekar, P. (2010). Influence of rare-earth ions on structural and magnetic properties of  $\text{CdFe}_2\text{O}_4$  ferrites. *Rare Metals*, 29(2), 168-173. <https://doi.org/10.1007/s12598-010-0029-z>
- [13] Silva, O., Lima, E. C. D., & Morais, P. C. (2003). Cadmium ferrite ionic magnetic fluid: Magnetic resonance in-

- vestigation. *Journal of applied physics*, 93(10), 8456-8458. <https://doi.org/10.1063/1.1540165>
- [14] Cai, C., Zhang, Z., Liu, J., Shan, N., Zhang, H., & Dionysiou, D. D. (2016). Visible light-assisted heterogeneous Fenton with ZnFe<sub>2</sub>O<sub>4</sub> for the degradation of Orange II in water. *Applied Catalysis B: Environmental*, 182, 456-468. <https://doi.org/10.1016/j.apcatb.2015.09.056>
- [15] Sharma, R., Bansal, S., & Singhal, S. (2015). Tailoring the photo-Fenton activity of spinel ferrites (MFe<sub>2</sub>O<sub>4</sub>) by incorporating different cations (M= Cu, Zn, Ni and Co) in the structure. *Rsc Advances*, 5(8), 6006-6018. <https://doi.org/10.1039/C4RA13692F>
- [16] Dhiman, M., Goyal, A., Kumar, V., & Singhal, S. (2016). Designing different morphologies of NiFe<sub>2</sub>O<sub>4</sub> for tuning of structural, optical and magnetic properties for catalytic advancements. *New Journal of Chemistry*, 40(12), 10418-10431. <https://doi.org/10.1039/C6NJ03209E>
- [17] Jadhav, S. D., Hankare, P. P., Patil, R. P., & Sasikala, R. (2011). Effect of sintering on photocatalytic degradation of methyl orange using zinc ferrite. *Materials letters*, 65(2), 371-373. <https://doi.org/10.1016/j.matlet.2010.10.004>
- [18] Garcia-Muñoz, P., Fresno, F., Peña O'Shea, V. A., & Keller, N. (2020). Ferrite materials for photoassisted environmental and solar fuels applications. *Heterogeneous Photocatalysis*, 107-162. [https://doi.org/10.1007/978-3-030-49492-6\\_4](https://doi.org/10.1007/978-3-030-49492-6_4)
- [19] Harish, K. N., Naik, H. B., Kumar, P. P., Vishwanath, R., & Kumar, G. Y. (2013). Optical and photocatalytic properties of CdFe<sub>2</sub>O<sub>4</sub> nanocatalysts: potential application in water treatment under solar light irradiation. *Archives of Applied Science Research*, 5(2), 42-51.
- [20] Patil, R. P., Pandav, R. S., Jadhav, A. V., Jadhav, S. D., & Hankare, P. P. (2016). Investigation of Structural, Magnetic and Photocatalytic Properties of Al Substituted Cobalt Ferrites. *Materials Focus*, 5(1), 11-16. <https://doi.org/10.1166/mat.2016.1293>
- [21] Mamba, G., & Mishra, A. K. (2016). Graphitic carbon nitride (g-C<sub>3</sub>N<sub>4</sub>) nanocomposites: a new and exciting generation of visible light driven photocatalysts for environmental pollution remediation. *Applied Catalysis B: Environmental*, 198, 347-377. <https://doi.org/10.1016/j.apcatb.2016.05.052>
- [22] Ombaka, L. M., Dillert, R., Robben, L., & Bahnemann, D. W. (2020). Evaluating carbon dots as electron mediators in photochemical and photocatalytic processes of NiFe<sub>2</sub>O<sub>4</sub>. *APL Materials*, 8(3), 031105. <https://doi.org/10.1063/1.5134432>
- [23] Ismael, M. (2021). Ferrites as solar photocatalytic materials and their activities in solar energy conversion and environmental protection: a review. *Solar Energy Materials and Solar Cells*, 219, 110786. <https://doi.org/10.1016/j.solmat.2020.110786>
- [24] Kefeni, K. K., & Mamba, B. B. (2020). Photocatalytic application of spinel ferrite nanoparticles and nanocomposites in wastewater treatment. *Sustainable materials and technologies*, 23, e00140. <https://doi.org/10.1016/j.susmat.2019.e00140>
- [25] Kubacka, A., Fernandez-Garcia, M., & Colon, G. (2012). Advanced nanoarchitectures for solar photocatalytic applications. *Chemical reviews*, 112(3), 1555-1614. <https://doi.org/10.1021/cr100454n>
- [26] Metal-Organic, V. F. A. B. *Research & Reviews: Journal of Material Sciences*. Vol (4) issue 2. 2016
- [27] Hankare, P. P., Kamble, P. D., Kadam, M. R., Rane, K. S., & Vasambekar, P. N. (2007). Effect of sintering temperature on the properties of Cu-Co ferrites prepared by oxalate precipitation method. *Materials Letters*, 61(13), 2769-2771. <https://doi.org/10.1016/j.matlet.2006.10.027>
- [28] Abbas, N., Rubab, N., Sadiq, N., Manzoor, S., Khan, M. I., Fernandez Garcia, J., ... & Yasmin, G. (2020). Aluminum-doped cobalt ferrite as an efficient photocatalyst for the abatement of methylene blue. *Water*, 12(8), 2285. <https://doi.org/10.3390/w12082285>
- [29] Ahmed, S. (2004). Photo electrochemical study of ferrioxalate actinometry at a glassy carbon electrode. *Journal of Photochemistry and Photobiology A: Chemistry*, 161(2-3), 151-154. [https://doi.org/10.1016/S1010-6030\(03\)00284-3](https://doi.org/10.1016/S1010-6030(03)00284-3)
- [30] Sadiq, M., Ali, M., Aman, R., Rashid, H. U., & Umar, M. N. (2015). Kinetic Study of Selective Gas-Phase Oxidation of Isopropanol to Acetone Using Monoclinic ZrO<sub>2</sub> as a Catalyst. *Química Nova*, 38, 891-895. <https://doi.org/10.5935/0100-4042.20150097>
- [31] Mahammed, B. A., & Ahmed, L. M. (2017). Enhanced photocatalytic properties of pure and Cr-modified ZnS powders synthesized by precipitation method. *Journal of Geoscience and Environment Protection*, 5(10), 101. <https://doi.org/10.4236/gep.2017.510009>
- [32] Liu, C., Zou, B., Rondinone, A. J., & Zhang, Z. J. (2000). Chemical control of superparamagnetic properties of magnesium and cobalt spinel ferrite nanoparticles through atomic level magnetic couplings. *Journal of the American Chemical Society*, 122(26), 6263-6267. <https://doi.org/10.1021/ja000784g>
- [33] Tsai, F. C., Ma, N., Chiang, T. C., Tsai, L. C., Shi, J. J., Xia, Y., ... & Chuang, F. S. (2014). Adsorptive removal of methyl orange from aqueous solution with crosslinking chitosan microspheres. *Journal of Water Process Engineering*, 1, 2-7. <https://doi.org/10.1016/j.jwpe.2014.02.001>
- [34] Xiaomeng, L., Jimin, X., Yuanzhi, S., & Jiamin, L. (2007). Surfactant-assisted hydrothermal preparation of submicrometer-sized two-dimensional BiFeO<sub>3</sub> plates and their photocatalytic activity. *Journal of materials science*, 42(16), 6824-6827. <https://doi.org/10.1007/s10853-006-1401-0>
- [35] Purkait, M. K., Maiti, A., Dasgupta, S., & De, S. (2007). Removal of congo red using activated carbon and its regeneration. *Journal of Hazardous Materials*, 145(1-2), 287-295. <https://doi.org/10.1016/j.jhazmat.2006.11.021>
- [36] Sakthivel, S., Neppolian, B., Shankar, M. V., Arabinodo, B., Palanichamy, M., & Murugesan, V. (2003). Solar photocatalytic degradation of azo dye: comparison of photocatalytic efficiency of ZnO and TiO<sub>2</sub>. *Solar energy materials and solar cells*, 77(1), 65-82. [https://doi.org/10.1016/S0927-0248\(02\)00255-6](https://doi.org/10.1016/S0927-0248(02)00255-6)
- [37] Ahmed, L. M. (2018). Photo-decolourization kinetics of acid red 87 dye in ZnO suspension under different types of UV-A light. *Asian J. Chem*, 30(9), 2134-2140. <https://doi.org/10.14233/ajchem.2018.21520>
- [38] Ahmed, L. M., & Hussein, F. H. (2012). Quantum yield of formaldehyde formation from methanol in the presence of TiO<sub>2</sub> and platinumized TiO<sub>2</sub> photocatalysts. In *Journal of Babylon University/Pure and Applied Sciences/College of Science/Babylon University Scientific Conference (Vol. 22, No. 1, pp. 464-470)*.
- [39] Zuafuani, S. I., & Ahmed, L. M. (2015). Photocatalytic decolorization of direct orange Dye by zinc oxide under UV irradiation. *Int. J. Chem. Sci*, 13(1), 187-196.
- [40] Mahammed, B. A., & Ahmed, L. M. (2017). Enhanced photocatalytic properties of pure and Cr-modified ZnS powders synthesized by precipitation method. *Journal of Geoscience and Environment Protection*, 5(10), 101. <https://doi.org/10.4236/gep.2017.510009>
- [41] Radović, M. D., Mitrović, J. Z., Kostić, M. M., Bojić, D. V., Petrović, M. M., Najdanović, S. M., & Bojić, A. L. (2015). Comparison of ultraviolet radiation/hydrogen peroxide, Fenton and photo-Fenton processes for the decolorization of reactive dyes. *Hemijiska industrija*, 69(6), 657-665. <https://doi.org/10.2298/HEMIND140905088R>
- [42] Ahmed, L. M., & Hussein, F. H. (2014). Roles of Photocatalytic Reactions of Platinumized TiO<sub>2</sub> Nanoparticles. LAP LAMBERT Academic Publishing.